

# Compression Mechanisms and Equations of State

R. J. Angel and N. L. Ross

*Phil. Trans. R. Soc. Lond. A* 1996 **354**, 1449-1459

doi: 10.1098/rsta.1996.0057

## Email alerting service

Receive free email alerts when new articles cite this article - sign up in the box at the top right-hand corner of the article or click [here](#)

To subscribe to *Phil. Trans. R. Soc. Lond. A* go to:  
<http://rsta.royalsocietypublishing.org/subscriptions>

# Compression mechanisms and equations of state

BY R. J. ANGEL<sup>1</sup> AND N. L. ROSS<sup>2</sup>

<sup>1</sup>*Bayerisches Geoinstitut, Universität Bayreuth, D-95440 Bayreuth, Germany*

<sup>2</sup>*Department of Geological Sciences, University College London, Gower Street, London WC1E 6BT, UK*

The derivations of equations of state to describe the volume–pressure variation of a solid are based upon certain assumptions about the properties of the solid. For finite strain equations of state, these assumptions include homogeneity and isotropy of the strain distribution in the sample, the continuous differentiability of the equation of state parameters with respect to extensive variables, and the assumption that terms involving higher-order powers of the finite strain do not contribute significantly to the free energy of the material. We examine these assumptions and demonstrate that, within the experimental uncertainties, crystalline solids with no or limited degrees of internal structural freedom compress in the manner predicted by finite strain equations of state, even though in some cases the assumptions involved in the derivation of the equation of state are demonstrably violated. In more complex structures with a larger number of degrees of structural freedom, a variety of behaviour is observed; most undergo continuous structural change with increasing pressure and the evolution of the volume with pressure again follows that predicted by the finite strain equations of state. However, a significant number of complex structures undergo changes in compression mechanism which, in some cases, result in significant deviations from the behaviour predicted by the equations of state.

## 1. Introduction

For a complete characterization of the structure, composition and dynamics of the Earth's interior it is necessary to have available the volume (or density) variations of candidate mantle minerals with pressure and temperature, otherwise termed the 'equation of state' (EOS) of the material. In addition, the calculation of phase equilibria in chemical systems at high pressures and temperatures also requires the use of the EOS of the phases in order to determine the volume changes associated with reactions and transformations. Such calculations are required not only to develop the pressure calibration of high-pressure apparatuses used to carry out experiments, but also to provide an independent cross-check on the positions of phase boundaries determined by such experiments. For most materials of relevance to the Earth's mantle, the EOS of the stable phases have only been determined to modest pressures, of the order of 5–10 GPa, at room pressure. Extrapolation of such data to the pressures and temperatures of the Earth's mantle is therefore often necessary. The question which we address in this paper is: to what extent are such extrapolations justified for typical mantle minerals?

*Phil. Trans. R. Soc. Lond. A* (1996) **354**, 1449–1459

*Printed in Great Britain*

1449

© 1996 The Royal Society

TeX Paper

## 2. Equations of state

The EOS most widely used to undertake extrapolations of the  $P$ – $V$  relations of minerals is the ‘Birch–Murnaghan’ (Birch 1947), which is based upon the fundamental assumption that the free energy of the solid may be expressed as a Taylor series in the Eulerian finite strain,  $\epsilon$ , defined as

$$2\epsilon = 1 - (V_0/V)^{2/3}, \quad (2.1)$$

where  $V_0$  is the ambient pressure volume of the material, and  $V$  the volume at elevated pressure. In its fourth-order form, the EOS is

$$P = \frac{3}{2}K_0f(1+2f)^{5/2}(1+\frac{3}{4}(K'_0-4)f+\frac{3}{8}(K_0K''_0+(K'-4)(K'-3)+\frac{35}{9})f^2), \quad (2.2)$$

where  $f = -\epsilon$  is the compression (a positive quantity). The third-order form is truncated at the term in  $f$ . A further truncation to a second-order expansion, by setting  $K'$  equal to 4, cannot be generally justified except for describing low-precision data.

In addition to the fundamental assumption noted above, the derivation of the Birch–Murnaghan EOS involves implicit assumptions about the properties of the solid under compression. First, the derivation assumes that the material under compression is isotropic, although Birch (1947) showed that (2.2) was also applicable to cubic materials. Second, it is assumed that the material under compression is homogeneously strained—that is that it behaves as an elastic continuum and all parts of the structure therefore compress at the same rate. This is clearly not the case in solids that consist not only of atoms and voids, but also contain atomic groupings and bonds of different compressibilities. Third, the termination of the Taylor series of the free energy in the finite strain implicitly assumes that the contribution from the higher powers of the finite strain are small compared to the low-order terms that give rise to (2.2) (see, for example, Jeanloz 1992; Anderson 1995). This condition also applies to any other EOS formalism that relies (explicitly or implicitly) upon series truncation (Anderson 1995). Lastly, it is assumed that the EOS parameters (in this case  $K$ ,  $K'$  and  $K''$ , which are themselves derivatives of  $V$  with respect to pressure) are continuously differentiable with respect to pressure, a requirement that is true for all EOS formalisms (Walzer *et al.* 1979). This has the obvious and well-known corollary that any EOS will not correctly describe the elastic properties of the material in the neighbourhood of, or through, a phase transition.

Despite the common violation of these assumptions, the Birch–Murnaghan EOS has been used widely and successfully to describe the  $P$ – $V$  relations of a wide number of materials under modest compression (that is to  $V/V_0$  of the order of 0.9). However, with the advent of more precise experimental data, we consider that it is now appropriate to explore once more the robustness of this EOS for extrapolating  $P$ – $V$  data of mantle minerals to the pressures of the Earth’s mantle. We test the Birch–Murnaghan EOS formalism by using direct determinations of the zero-pressure bulk modulus and its pressure derivatives (obtainable from elasticity measurements at low pressures) in the EOS to predict the  $P$ – $V$  relationship of various minerals at higher pressures. These predictions are then compared with pressure-volume data determined directly by a variety of *in situ* diffraction techniques at high pressures. For those cases where the comparison indicates a failure in the EOS, single-crystal high-pressure diffraction measurements can reveal the underlying structural reasons for the failure. In this way the practical limits to the application of EOSs, in terms

of structural complexity, can begin to be assessed. We note here that we restrict ourselves, in the main, to the discussion of the room temperature behaviour of minerals because this is the regime for which the most precise data is available. We also note that, although we explicitly consider the Birch–Murnaghan EOS, our conclusions are equally applicable to many other common EOS formalisms, since most are indistinguishable in the compression range of interest (Jeanloz 1988; Anderson 1995).

### 3. Structural compression

#### (a) *Invariant lattice complexes*

Some crystal structures possess no degrees of internal freedom because all of the atoms occupy special equivalent positions or symmetry sites within the unit cell so that there are no variable atomic coordinates. The internal geometry of these structures, including all of the interatomic distances and angles, is then completely defined by the value(s) of the unit-cell parameter(s). Such structures are properly termed ‘invariant lattice complexes’ (Fischer & Koch 1987) but here they will be referred to as ‘fixed’ structures. In cubic fixed structures the ratio of every interatomic distance to the cell edge is fixed. It then follows that, upon compression, all distances within the structure are strained by the same amount. Such cubic fixed structures therefore meet the criteria of undergoing homogeneous strain upon compression and, given that there are no degrees of structural freedom and no discontinuities in the pair-wise interatomic potentials, one would expect that the compression of all such structures to be adequately described by finite strain EOSs.

This is indeed observed to be the case for the extensive data for the oxides and halides with the NaCl structure. For example, the sound velocities of MgO have been measured by a spectroscopic technique to pressures in excess of 20 GPa (Chopelas 1992), and these data indicate that there are no significant discontinuities or changes in behaviour in MgO over this pressure range. Furthermore, this data is in excellent agreement with the extrapolation, through the Birch–Murnaghan EOS, of the ultrasonic data to 3 GPa (Jackson & Niesler 1982). To demonstrate that the success of the finite strain formalism in fixed structures is not restricted to diatomic NaCl-structured solids we perform a similar comparison exercise for CaF<sub>2</sub>, fluorite. The fluorite structure has *Fm*3*m* symmetry with the Ca occupying four-fold sites at (0,0,0) with *m* – 3*m* symmetry and the F occupying eight-fold sites at  $\pm(\frac{1}{4}, \frac{1}{4}, \frac{1}{4})$  with  $-43m$  symmetry. Figure 1 shows the excellent agreement between the unit-cell volumes determined *in situ* at high pressures by single-crystal diffraction to 8 GPa by Angel (1992) and the volumes predicted by using the Birch–Murnaghan formalism to extrapolate the elastic moduli which were measured by ultrasonic techniques to a maximum pressure of only 0.4 GPa by Wong & Schuele (1968). There are many more examples of experimental data that demonstrate that cubic ‘fixed structures’ (we have been unable to locate any high-pressure data for non-cubic examples) obey the Birch–Murnaghan EOS over wide ranges of pressures.

#### (b) *Partially fixed structures*

A number of structures that can be considered to be derived from close-packed anion arrays through the filling of some of the tetrahedral and octahedral interstices with cations have high symmetry and very few internal degrees of freedom. For example, the spinel structure (based upon cubic-close-packing of the anions) has one

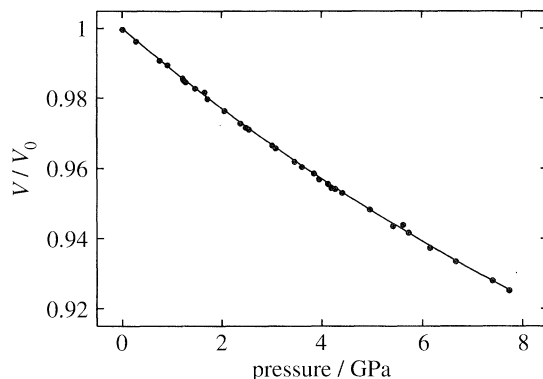


Figure 1. The volume–pressure variation of  $\text{CaF}_2$  (data points) as determined by X-ray diffraction (Angel 1992) compared to the Birch–Murnaghan EOS (line) derived from ultrasonic measurements of  $K$  and  $K'$  to a maximum pressure of 0.4 GPa by Wong & Schuele (1968).

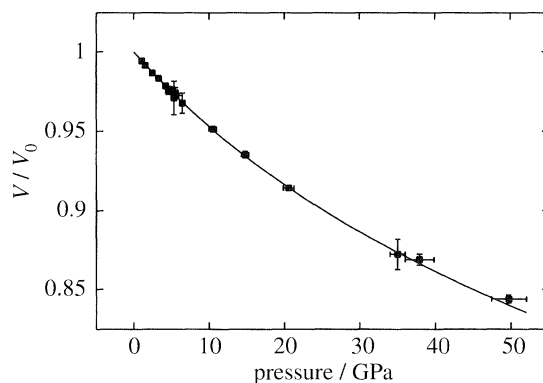


Figure 2. Volume–pressure variation of  $(\text{Fe,Mg})_2\text{SiO}_4$  spinel (data points with estimated errors) determined by X-ray diffraction (Zerr *et al.* 1993) compared to the Birch–Murnaghan EOS (line) derived from Brillouin spectroscopy measurements of  $K_0$  (Weidner *et al.* 1984) and from ultrasonic measurements of  $K'$  (Rigden *et al.* 1991).

internal structural coordinate, the positional parameter of the oxygen, the variation of which controls the relative sizes of the tetrahedral and octahedral cation sites (see, for example, Brown 1982). There is no *a priori* reason why this parameter should remain constant or vary smoothly with compression of the cell edge (or equivalently the cell volume) which determines the absolute size of the cation–oxygen separations. In  $\text{Ni}_2\text{SiO}_4$  spinel, the oxygen parameter changes with pressure so as to increase the Ni–O distances at the expense of the Si–O distances (Finger *et al.* 1979). Despite this possibility of inhomogeneous strain within the structure, experiments to much higher pressures on  $(\text{Mg,Fe})_2\text{SiO}_4$  spinel show excellent agreement (figure 2) between the volume–pressure data collected by Zerr *et al.* (1993) and the lower pressure determinations of  $K$  and  $K'$  by Brillouin spectroscopy (Weidner *et al.* 1984) and ultrasonics (Rigden *et al.* 1991). Furthermore, the smooth variation of the Raman bands with pressure (Chopelas *et al.* 1994) indicate that there is no change in compression mechanism within  $\text{Mg}_2\text{SiO}_4$  spinel, at least to 20 GPa.

The structure of corundum,  $\text{Al}_2\text{O}_3$ , is based upon hexagonal packing of anions with alumina filling the octahedral interstices. The aluminium and oxygen positions in the structure each possess a single variable structural coordinate which can vary



independently of the cell parameters to modify both the Al–O bond lengths and the angular distortion of the  $\text{AlO}_6$  octahedron. However, full single-crystal structure determinations to pressures of *ca.* 5 GPa (Finger & Hazen 1978) and 8.6 GPa (d'Amour *et al.* 1978) show that there is no significant change in these internal coordinates, while the  $c/a$  ratio remains constant to *ca.* 50 GPa (Richet *et al.* 1988) and all of the available volume data in this pressure range can be fitted by a single Birch–Murnaghan EOS.

The rutile structure type is another example of a non-cubic structure with a single variable internal coordinate, in this case the anion  $x$ -parameter. Single-crystal structural studies by Ross *et al.* (1990) to 15.8 GPa on the  $\text{SiO}_2$  polymorph with this structure (the mineral stishovite) show that it undergoes inhomogeneous internal strain as a result of the internal coordinate remaining constant while the tetragonal  $c/a$  ratio increases with pressure. Figure 3 shows that at low pressures there is good agreement between the single-crystal compression data and that calculated with a third order finite strain EOS using the values of  $K_0$  from Brillouin scattering (Weidner *et al.* 1982) and  $K'$  from ultrasonic measurements to 3 GPa (Rigden *et al.* 1994). At higher pressures there appears to be a systematic divergence of the two sets of data that is in excess of the experimental uncertainties of the diffraction experiment. This discrepancy might initially be attributed to the failure of the finite-strain EOS under conditions of non-homogeneous strain within the crystal structure. However, careful assessment of the uncertainties in  $K_0$ , due to the conversion of the measured adiabatic bulk modulus to its isothermal equivalent (the conversion factor  $\alpha\gamma T$  has been assumed to be of the order of 1–2%), the uncertainty in  $K'$  and the possibility that  $K''$  may be as much as  $-0.15 \text{ GPa}^{-1}$  and not be detected in the ultrasonic experiments (Niesler 1986), indicates that the discrepancy may not be significant (figure 3). This example serves to highlight the precision to which both  $P$ – $V$  data and elastic moduli need to be measured in order to provide definitive tests of EOS formalisms in hard materials such as stishovite. In summary, current experimental data are not inconsistent with the conclusion that structures in which there are few degrees of internal freedom still follow finite-strain behaviour upon compression, even though they undergo significant amounts of inhomogeneous strain.

### (c) Fully variable structures

Continuing the theme of structures derived from close-packing of anions, we now consider two much more complex structures with a large number of internal structural degrees of freedom. Single-crystal structural studies show that these undergo significant internal inhomogeneous strain upon compression, as well as changes in compression mechanism; both effects which might be expected to affect the applicability of the Birch–Murnaghan EOS formalism.

The first example is the olivine structure, which is based upon a distorted hexagonal array of anions with some tetrahedral interstices filled with Si and the octahedral interstices partially filled with +2 cations such as Mg, Fe, Co, etc. The distortion of the hexagonal close packing of the oxygens, together with the distribution of the cations, reduces the unit cell to orthorhombic symmetry and only the position of the M1 site is completely fixed within the structure. Therefore, all interatomic distances and angles, except those involving only the M1 cations, are variable independently of the changes in unit-cell parameters.

Single-crystal structure determinations have been performed to 14.9 GPa on  $\text{Mg}_2\text{SiO}_4$  (Kudoh & Takeuchi 1985) and to *ca.* 8 GPa on  $\text{Co}_2\text{SiO}_4$  (Ross 1993). Both

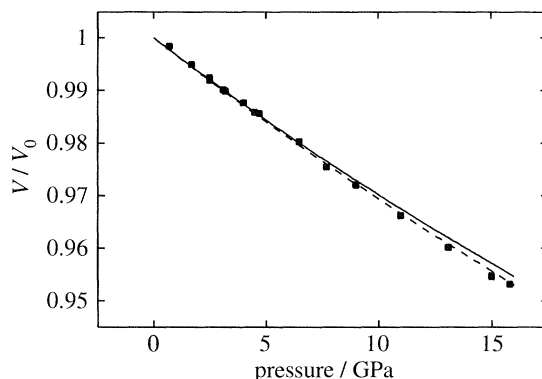


Figure 3. Volume–pressure variation of  $\text{SiO}_2$  stishovite (data points) determined by X-ray diffraction (Ross *et al.* 1990) compared to the Birch–Murnaghan EOS (solid line) derived from Brillouin spectroscopy measurements of  $K_0$  (Weidner *et al.* 1982) and from ultrasonic measurements of  $K'$  (Rigden *et al.* 1994). The dashed line indicates a lower bound for a fourth-order Birch–Murnaghan EOS. The parameters used are  $K_T = 300$  GPa,  $K' = 4.9$  and  $K'' = -0.15$   $\text{GPa}^{-1}$ .

of these studies demonstrate that as pressure is increased the changes in internal coordinates give rise to differential compression of the two metal–oxygen octahedra compared to the  $\text{SiO}_4$  tetrahedra. Both structures also display a distinct change in compression mechanism, whereby the M1 octahedra ceases to undergo compression, at *ca.* 6 GPa for  $\text{Co}_2\text{SiO}_4$  and between 8 and 9 GPa in  $\text{Mg}_2\text{SiO}_4$  (figure 4). This change in compression behaviour of  $\text{Mg}_2\text{SiO}_4$  olivine is also reflected in the changes at 8–9 GPa in the slope of a number of Raman bands with pressure (Chopelas 1990, Wang *et al.* 1993). It may also be the cause of the anomalous behaviour of the  $c_{55}$  elastic constant (Webb 1989) of natural olivine, especially pronounced at pressures above *ca.* 8 GPa (Zaug *et al.* 1993). The unit-cell parameter data for  $\text{Co}_2\text{SiO}_4$  do not extend far enough beyond the pressure at which the change in compression mechanism occurs to allow the effect upon the EOS to be evaluated. But the cell parameters of  $\text{Mg}_2\text{SiO}_4$  show distinct changes in slope around 8 GPa (Kudoh & Takeuchi 1985), although it is not clear from the data whether there is an associated change in the slope of volume with pressure. It should be noted that all of these experimental studies clearly show that this change in compression mechanism is not accompanied by a symmetry change so, in combination with the evidence that there is no associated significant discontinuity in the volume, this behaviour does not constitute a phase transition.

A further, and more distinct, example is provided by the high-pressure behaviour of  $\text{MgSiO}_3$  orthopyroxene, another structure loosely based upon an anion arrangement that can be considered a distortion of a hexagonal-close-packed array. As for olivine, Si occupies tetrahedral interstices and the Mg octahedral interstices, but the arrangement of these is such that the structure is best considered as bands of octahedra cross-linked by single corner-sharing tetrahedral chains. The structure is therefore much more open than the structures that we have previously discussed and, since none of the ten symmetry independent atoms occupy fixed positions, it possesses a large number of internal degrees of freedom. The most striking feature of the variation of the volume with pressure (Angel & Hugh-Jones 1994) is a change in the slope at *ca.* 4.2 GPa (figure 5). The lower pressure regime is described by an EOS with a large  $K'$  of  $15 \pm 2$ , and a bulk modulus of  $95.8 \pm 3.0$  GPa, whereas the

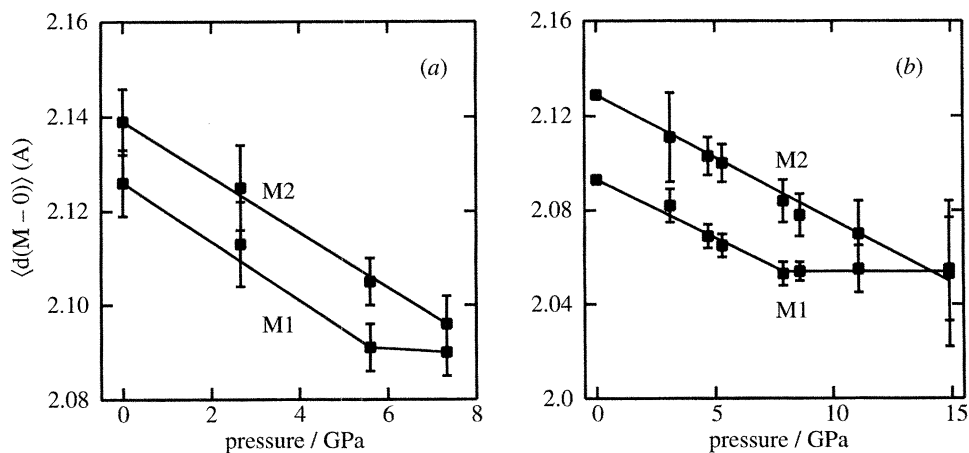


Figure 4. Variation with pressure of the mean bond-lengths of the two independent cation octahedra in (a)  $\text{Co}_2\text{SiO}_4$  (Ross 1993) and (b)  $\text{Mg}_2\text{SiO}_4$  (Kudoh & Takeuchi 1985) olivines.

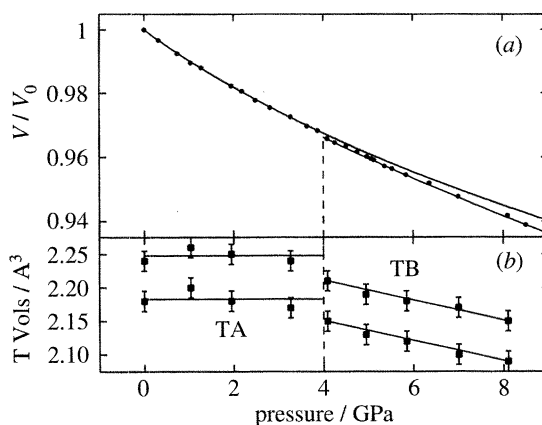


Figure 5. Volume–pressure variation of  $\text{MgSiO}_3$  orthopyroxene (a) showing the change in EOS at *ca.* 4 GPa, and the accompanying initiation of significant compression of the  $\text{SiO}_4$  tetrahedra (b). All data from Hugh-Jones & Angel (1994).

higher-pressure data are fitted by a Birch–Murnaghan EOS with  $K' = 5.6 \pm 2.9$  and  $K = 123 \pm 16$  GPa (Hugh-Jones & Angel 1994; Angel & Hugh-Jones 1994a). Careful X-ray diffraction experiments showed that there is no change in space group symmetry accompanying this change in behaviour, a conclusion reinforced by the Raman data which show changes in the pressure dependencies of most of the Raman bands at this pressure but no change in the number of bands (Chopelas & Boehler 1991). The change in compressibility of the structure as a whole is due to a clear change in compression mechanism at *ca.* 4.2 GPa. Below this pressure the  $\text{SiO}_4$  tetrahedra display no significant volume change, while volume reduction is accommodated by tetrahedral rotation and compression of the two  $\text{MgO}_6$  octahedra. Above 4.2 GPa the tetrahedra show significant compression (figure 5), the change with increasing pressure of the tilts and rotation of the tetrahedra are reversed from that at lower pressures, and the  $\text{MgO}_6$  octahedra compress at a reduced rate (Hugh-Jones & Angel 1994).

Experimental data from single-crystal diffraction studies of a limited number of



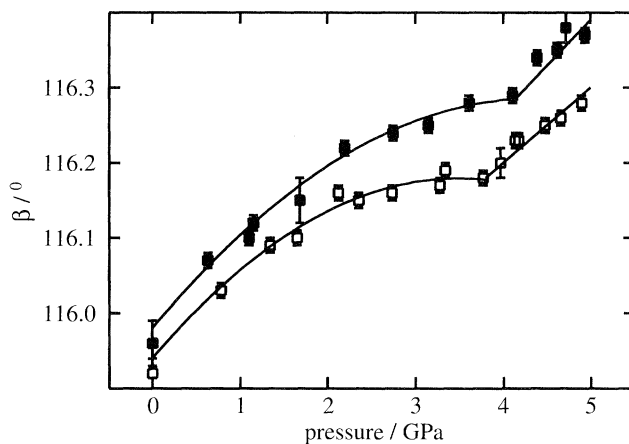


Figure 6. The variation with pressure of the  $\beta$  unit-cell angle of two microcline samples of slightly different compositions (Hackwell 1994).

other minerals at high pressures are also suggestive of similar changes in compression mechanism without volume discontinuities. The structures of feldspars consist of an open framework of  $\text{SiO}_4$  and  $\text{AlO}_4$  corner-linked tetrahedra with larger cations, such as Na, K, and Ca, occupying the larger cavities within the framework. The symmetry of the structures is, at maximum,  $C2/m$ , but at room temperature the symmetry of Al,Si ordered feldspars with these compositions are triclinic, and the positions of all of the atoms within the unit cell are completely unconstrained. A compression study of ordered K-rich alkali feldspars (microcline) shows that the unit-cell angles undergo reversals of their lower pressure trends at pressures between 3.5 and 4 GPa (figure 6), the pressure at which this occurs depending upon the composition (Hackwell 1994). Simultaneous high-pressure high-temperature diffraction measurements upon anorthite ( $\text{CaAl}_2\text{Si}_2\text{O}_8$  feldspar) reveals that the high-temperature I-1 structure also displays distinct changes of unit-cell parameters under compression, which are believed to correspond to a rapid change in the conformation of the tetrahedral framework over an extremely limited pressure range (Hackwell & Angel 1995; Christy & Angel 1995). In both microcline and anorthite the cell parameter changes are not accompanied by either a symmetry change or a volume discontinuity. Current data are not of sufficient precision, however, to determine whether these rapid changes in structural conformation with pressure lead to structures with significantly different volume derivatives with respect to pressure.

Finally, we note the case of orthorhombic  $\text{MgSiO}_3$  perovskite, for which single-crystal data (Ross & Hazen 1990) suggests that it undergoes a change in compression mechanism at *ca.* 5 GPa at room temperature. Below this pressure, volume reduction is accommodated by reduction in the Si–O bond lengths within the  $\text{SiO}_6$  octahedra, and above this pressure by tilting of the octahedra about their common oxygens. The precision of the available volume–pressure measurements of  $\text{MgSiO}_3$  perovskite (see, for example, Mao *et al.* 1991) is not sufficient to determine whether any subtle changes in the volume–pressure relationship accompanies this change in compression mechanism. Unfortunately, the Raman spectra of  $\text{MgSiO}_3$  perovskite measured from 7.5 to *ca.* 45 GPa by Chopelas & Boehler (1992) could not be followed in the 0–7.5 GPa pressure range, so independent confirmation of a compression mechanism

change through changes in rates of band shifts with pressure (as observed for orthopyroxenes) is not yet available.

#### 4. Conclusions

It is clear from our brief review, and from extensive previous work, that the  $P$ - $V$  relationships of simple solids with no degrees of internal structural freedom follow the Birch–Murnaghan EOS over a wide range of pressure (and hence compression). We have also demonstrated that this EOS also appears to be suitable for the description of the compression of a large number of solids with structures that possess a few degrees of internal freedom and which therefore do not strictly meet the assumptions of homogeneous strain or isotropy necessary for its derivation. Therefore, the  $P$ - $V$  behaviour of such simple solids can be reliably extrapolated to high pressures (and temperatures), provided there are no phase transitions.

By contrast, complex solids that possess significant degrees of structural freedom display a variety of behaviour. The majority, despite violating the conditions of isotropy and homogeneous strain, still display  $P$ - $V$  relationships that are described by the Birch–Murnaghan EOS. There are a number of other major mantle minerals that, in addition, also undergo changes in compression mechanism at high pressures without any detectable deviation in the  $P$ - $V$  relationship predicted by the Birch–Murnaghan EOS. Examples of such minerals include olivines,  $\text{MgSiO}_3$  perovskite and microcline feldspar. Finally, minerals such as  $(\text{Mg,Fe})\text{SiO}_3$  orthopyroxenes display distinct changes in the mechanism of compression at modest pressures that lead to significant deviations from the behaviour predictable by a single EOS (figure 5). The compression behaviour of most mantle minerals can therefore only be safely predicted by the extrapolation of low-pressure measurements if it is known that they do not undergo compressional mechanism changes at higher pressures.

The examples that we have given above clearly demonstrate that changes in compression mechanism occur in structures which have sufficient degrees of internal freedom. There are not, however, enough examples of such behaviour known to be able to determine what the term ‘sufficient degrees of freedom’ actually means in quantitative terms. It is also clear that this is not the only factor that determines whether such mechanism changes occur upon compression. For example, the fact that  $(\text{Fe,Mg})\text{SiO}_3$  orthopyroxenes undergo a fairly abrupt change in compression mechanism at *ca.* 4 GPa indicates that this structure type possesses the necessary degrees of freedom. But orthopyroxenes containing a small amount of Ca substituted for  $(\text{Mg} + \text{Fe})$  display no such abrupt change (Angel & Hugh-Jones 1994b) and the  $P$ - $V$  data collected to greater than 6 GPa is in excellent agreement with that predicted by the EOS parameters determined from ultrasonic measurements to 3 GPa (Webb & Jackson 1993). Neither can simple predictive tools such as the ‘packing fraction’ of the structure (see Anderson 1995) account for such behaviour.

One of the factors that does seem to contribute to changes in compression mechanism is the presence within the structure of some longer and/or weaker cation–oxygen bonds that are differentially compressed when the more rigid units within the structure rotate upon initial compression. Thus, the longest Mg–O bonds in the orthoenstatite structure are initially compressed quite rapidly by rotation of the tetrahedra (Hugh-Jones & Angel 1994), while it is clear that in feldspars, initial compression must occur by flexing of the framework that pushes the oxygen atoms that bridge the tetrahedra out into the cavities occupied by cations of low charge and

large radius (Angel 1994). We would speculate that the observed changes in compression mechanism are related to these cation–oxygen bonds playing an initially passive role during compression, but, upon shortening, the rapidly increasing cation–anion repulsions force the framework to take up a new mode of compression. Testing of this speculation must await the accumulation of much more high-precision structural data on such crystalline solids.

We thank S. L. Webb, A. Chopelas, S. L. Rigden and A. Jephcoat for comments and discussions of this contribution. D. A. Hugh-Jones and T. P. Hackwell collected much of the experimental diffraction data on the pyroxenes and feldspars that we have discussed.

## References

- Anderson, O. L. 1995 *Equations of state of solids for geophysics and ceramic science*. Oxford University Press.
- Angel, R. J. 1992 The high-pressure, high-temperature equation of state of calcium fluoride,  $\text{CaF}_2$ . *J. Phys. Cond. Matter* **5**, L141–L144.
- Angel, R. J. 1994 Feldspars at high pressure. In *Feldspars and their reactions* (ed. I. Parsons), pp. 271–312. Dordrecht: Kluwer.
- Angel, R. J. & Hugh-Jones, D. A. 1994a Equations of state and thermodynamic properties of enstatite pyroxenes. *J. Geophys. Res.* **99**, 19 777–19 783.
- Angel, R. J. & Hugh-Jones, D. A. 1994b The effect of Fe on the compression of orthopyroxenes. *Eos* **75**, 605.
- Birch F. 1947 Finite strain of cubic crystals. *Phys. Rev.* **71**, 809–824.
- Brown, G. E. 1982 Olivine and silicate spinels. *M. S. A. Rev. Mineralogy* **5**, 275–392.
- Chopelas, A. 1990 Thermal properties of forsterite at mantle pressures derived from vibrational spectroscopy. *Phys. Chem. Minerals* **17**, 149–156.
- Chopelas, A. 1992 Sound velocities of  $\text{MgO}$  to very high compression. *Earth Planet. Sci. Lett.* **114**, 185–192.
- Chopelas, A. & Boehler, R. 1991 Raman spectroscopy of high-pressure  $\text{MgSiO}_3$  phases synthesised in a  $\text{CO}_2$  laser heated diamond anvil cell. *Terra Abstr.* **3**, 68.
- Chopelas, A. & Boehler, R. 1992 Raman spectroscopy of high-pressure  $\text{MgSiO}_3$  phases synthesised in a  $\text{CO}_2$  laser heated diamond anvil cell: perovskite and clinopyroxene. In *High pressure research in geophysics* (ed. M. H. Manghnani & S. Akimoto), pp. 98–113. Tokyo: Center of Academic Publications Japan.
- Chopelas, A., Boehler, R. & Ko, T. 1994 Thermodynamics and behaviour of  $\gamma\text{-Mg}_2\text{SiO}_4$  at high pressure: implications for  $\text{Mg}_2\text{SiO}_4$  phase equilibrium. *Phys. Chem. Minerals* **21**, 351–359.
- Christy, A. G. & Angel, R. J. 1995 A model for the origin of cell-doubling phase transitions in clinopyroxene and body-centered anorthite. *Phys. Chem. Minerals* **22**, 129–135.
- d'Amour, H., Schiferl, D., Denner, W., Schulz, H. & Holzapfel, W. B. 1978 High-pressure single-crystal structure determinations for ruby up to 90 kbar using an automatic diffractometer. *J. Appl. Phys.* **49**, 4411–4416.
- Finger, L. W. & Hazen, R. M. 1978 Crystal structure and compression of ruby to 46 kbar. *J. Appl. Phys.* **49**, 5822–5826.
- Finger, L. W., Hazen, R. M. & Yagi, T. 1979 Crystal structures and electron densities of nickel and iron silicate spinels at elevated temperature or pressure. *Am. Miner.* **64**, 1002–1009.
- Fischer, W. & Koch, E. 1987 Lattice complexes. In *International tables for crystallography* (ed. T. Hahn), vol. A, pp. 825–854. Dordrecht: Reidel.
- Hackwell, T. P. 1994 The structural behaviour of aluminosilicate frameworks at high pressures and temperatures. Ph.D. thesis, University of London.
- Hackwell, T. P. & Angel, R. J. 1995 Reversed brackets for the  $P - 1 \rightleftharpoons I - 1$  transition in anorthite at high pressures and temperatures. *Am. Miner.* **80**, 239–246.
- Hugh-Jones, D. A. & Angel, R. J. 1994 A compressional study of  $\text{MgSiO}_3$  orthoenstatite up to 8.5 GPa. *Am. Miner.* **79**, 405–410.

- Jackson, I. & Niesler, H. 1982 The elasticity of periclase to 3 GPa and some geophysical implications. In *High pressure research in geophysics* (ed. M. H. Manghnani & S. Akimoto), pp. 98–113. Tokyo: Center of Academic Publications Japan.
- Jeanloz, R. 1988 Universal equation of state. *Phys. Rev. B* **38**, 805–807.
- Jeanloz, R. 1992 Differential finite-strain equations of state. In *High pressure research in geophysics* (ed. M. H. Manghnani & S. Akimoto), pp. 147–156. Tokyo: Center of Academic Publications Japan.
- Kudoh, Y. & Takeuchi, Y. 1985 The crystal structure of forsterite  $\text{Mg}_2\text{SiO}_4$  under high pressure up to 149 kb. *Z. Kristallogr.* **171**, 291–302.
- Mao, H. K., Hemley, R. J., Fei, Y., Shu, J.-F., Chen, L. C., Jephcoat, A. P. & Wu, Y. 1991 Effect of pressure, temperature and composition on lattice parameters and density of  $(\text{Fe,Mg})\text{SiO}_3$ -perovskites to 30 GPa. *J. Geophys. Res.* **96**, 8069–8079.
- Niesler, H. 1986 A new technique for the measurement of elastic wave velocities on jacketed polycrystals at high pressure. M.Sc. thesis, Australian National University.
- Richet, P., Xu, J.-A. & Mao, H.-K. 1988 Quasi-hydrostatic compression of ruby to 500 kbar. *Phys. Chem. Minerals* **16**, 207–211.
- Rigden, S. M., Gwanmesia, G. D., FitzGerald, J. D., Jackson, I. & Liebermann, R. C. 1991 Spinel elasticity and seismic structure of the transition zone of the mantle. *Nature* **354**, 143–145.
- Rigden, S. M., Li, B. & Liebermann, R. C. 1994 Elasticity of stishovite at high pressures. *Eos* **75**, 596.
- Ross, N. L. 1993 High-pressure behaviour of the  $\text{Co}_2\text{SiO}_4$  polymorphs. *Terra Abstr.* **5**, 499.
- Ross, N. L. & Hazen, R. M. 1990 High-pressure crystal chemistry of  $\text{MgSiO}_3$  perovskite. *Phys. Chem. Minerals* **17**, 228–237.
- Ross, N. L., Shu, J.-F., Hazen, R. M. & Gasparik, T. 1990 High-pressure crystal chemistry of stishovite. *Am. Miner.* **75**, 739–747.
- Walzer, U., Ullmann, W. & Pan'kov, V. L. 1979 Comparison of some equation-of-state theories by using experimental high-compression data. *Phys. Earth Planet. Int.* **18**, 1–12.
- Wang, S. Y., Sharma, S. K. & Cooney, T. F. 1993 Micro-Raman and infra-red spectral study of forsterite under high pressure. *Am. Miner.* **78**, 469–476.
- Webb, S. L. 1989 The elasticity of the upper mantle orthosilicates olivine and garnet to 3 GPa. *Phys. Chem. Minerals* **16**, 684–692.
- Webb, S. L. & Jackson, I. 1993 The pressure dependence of the elastic moduli of single-crystal orthopyroxene  $(\text{Mg}_{0.8}\text{Fe}_{0.2})\text{SiO}_3$ . *Eur. J. Mineral.* **5**, 1111–1120.
- Weidner, D. J., Bass, J. D., Ringwood, A. E. & Sinclair, W. 1982 The single-crystal elastic moduli of stishovite. *J. Geophys. Res.* **87**, 4740–4746.
- Weidner, D. J., Sawamoto, H., Sasaki, S. & Kumazawa, M. 1984 Single-crystal elastic properties of the spinel phase of  $\text{Mg}_2\text{SiO}_4$ . *J. Geophys. Res.* **89**, 7852–7860.
- Wong, C. & Schuele, D. E. 1968 Pressure and temperature derivatives of the elastic constants of  $\text{CaF}_2$  and  $\text{BaF}_2$ . *J. Phys. Chem. Solids* **29**, 1309–1330.
- Zaug, J. M., Abramson, E. H., Brown, J. M. & Slutsky, L. J. 1993 Sound velocities in olivine at Earth mantle pressures. *Science* **260**, 1487–1489.
- Zerr, A., Reichmann, H., Euler, H. & Boehler, R. 1993 Hydrostatic compression of  $\gamma$ - $(\text{Mg}_{0.6}\text{Fe}_{0.4})\text{SiO}_4$  to 50.0 GPa. *Phys. Chem. Minerals* **19**, 507–509.